

## DESIGN AND PERFORMANCE OF A SOLAR GENERATOR WITH MAXIMUM POWER POINT TRACKING

Daniel L. Meier<sup>1</sup> and Brian J. Meier<sup>2</sup>

<sup>1</sup>Lightdrop Harvest, LLC, 693 Center Street, St. Marys, PA 15857, USA

<sup>2</sup>Richardson Cooling Packages, LLC, 731 Moravia Street, New Castle, PA 16101, USA

**ABSTRACT:** A small solar generator system, with power-matched components, has been designed and tested. The system consists of a 255 W module with 60 crystalline silicon cells in series (156 mm), feeding a charge controller with maximum power point tracking capable of delivering 20 A of charging current to a 12 V, 100 Ah (1200 Wh of energy) deep-cycle lead-acid battery, which powers a 1500 W pure sine wave inverter. The power efficiencies of the charge controller (PV in to battery out) and the inverter (battery in to AC out) were measured to be 90% and 93%, respectively, for a total system efficiency (PV in to AC out) of 84%. An AC-powered battery charger is also provided to automatically supplement the PV charge controller, as needed. The module can be mounted on a vertical wall, with a tilt mechanism which allows a choice of discrete tilt angles for different seasons. The system is expandable up to eight modules and charge controllers for significantly increased energy production and storage. A heat transfer analysis suggests the module power output can be increased by 6% (relative) if passive cooling fins are applied to the back of the module.

**Keywords:** Stand-alone PV Systems, Energy Performance, Battery Storage and Control, Silicon, System Performance

### 1 INTRODUCTION

This work follows others [1], [2] and seeks to provide the design basis for a balanced choice of components for a small stand-alone solar generator, to present operational data for the system, and to examine prospects for improving system performance by passively cooling the solar module. Such a solar generator is well-matched to the power requirements of a home office, a tool shed, or to provide emergency power to critical loads. Charging a 12 V battery typically requires a specialized module with 36 cells in series along with a switching shunt regulator, for example. This work employs a standard 60-cell module (common in multi-MW PV installations and available at  $< \$1/W_p$ ) along with a charge controller having maximum power point tracking (MPPT) which approximately doubles the charging current relative to that of the module alone. In addition, a mechanism is incorporated which allows the module to be mounted on a vertical surface (e.g., house wall) with a provision for tilting at discrete angles to better intercept sunlight during different seasons. Finally, the prospect of increasing module output by passive cooling is examined.

### 2 SYSTEM DESIGN

A block diagram of the full solar generator system is given in Fig. 1, with energy extracted from sunlight flowing through to the AC load.

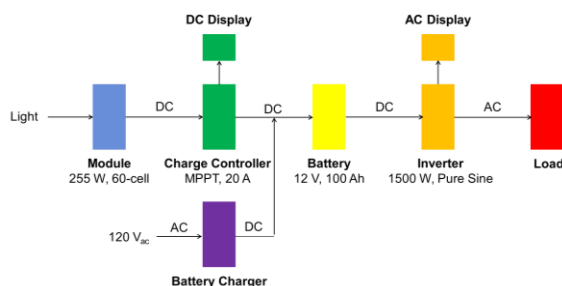


**Figure 1:** Block diagram of the solar generator system.

#### 2.1 Components

Key components of the system are given in Table I. The battery is the central element of the system, as it stores the electrical energy from the PV module and dispenses that energy to the inverter. A sealed 12 V deep-cycle lead-acid battery with absorbent glass mat (AGM) technology from Concorde Battery Corporation with a capacity of 100 Ah was chosen. This battery can accept charging currents in the 20 – 80 A range. A fully charged battery could then theoretically supply 1200 Wh of energy if taken to complete discharge. This matches well with a 255 W, 60-cell crystalline silicon module from Suniva. With average daily solar insolation of 4.2 kWh/m<sup>2</sup> (4.2 h of 1-sun equivalent) [3], the module will produce 1070 Wh of energy on average (standard test conditions). This is 89% of the energy storage capacity of the battery, and so would allow up to 89% average depth of battery discharge each day. However, with such a deep discharge, the expected life cycles of the battery would be only 450 (1.2 years). To prolong the useful life of the battery, the system is instead designed for a 50% depth of discharge (50 Ah, 600 Wh), for which the expected life cycles is 1000 (2.7 years).

**Table I:** Key components of solar generator system.

Component	Vendor	Model
Module	Suniva	OPT255-60-4-100 (255 W)
Controller	Blue Sky	Solar Boost 2512iX-HV
DC Display	Blue Sky	IPN-ProRemote
Battery	Concorde	GPL-27T (100 Ah, AGM)
Inverter	Samlex	PST-150S-12A
AC Display	P3 Int'l	Kill-A-Watt P4400
Charger	Husky	HSK072HD (12V, 6A)

A 1500 W true sine wave inverter with 3000 W surge capability from Samlex was chosen to cover typical loads. The additional inverter power capability is needed to supply starting power, such as in-rush current to a motor. Pure sine wave (as opposed to modified sine wave) provides clean power for even sensitive devices such as laser printers. The AC display provides instantaneous  $I_{ac}$ ,  $V_{ac}$ ,  $P_{ac}$  as well as cumulative kWh<sub>ac</sub>.

The charge controller from Blue Sky Energy is compatible with 60-cell modules up to 270 W, employs MPPT for maximum power transfer from module to battery, and delivers up to 20 A of charging current. The DC display provides a variety of module and charge controller information, including  $I_{dc}$  and  $V_{dc}$  values.

A supplementary battery charger from Husky is linked to the battery voltage, so that it only delivers charging current when PV charging is inadequate. Typically, the battery voltage must fall below 11 V (programmable value) before the supplementary charger is triggered. A relay that is energized from the charge controller connects the supplementary charger into the system. The battery can be charged from both the charge controller and the battery charger simultaneously.

2.2 Module Wall Mount

In a typical residential PV installation, the modules are mounted on the roof. However, for a simple stand-alone system, the module may be mounted on a vertical wall for versatility, or may be free-standing. A module wall mount, illustrated in Fig. 2, was designed for this purpose. The module can be tilted away from the wall by means of a hinge and a tilt bar which slips over a pair of pins to define and stabilize the tilt angle. In this way the tilt angle can be changed season-by-season to maximize the amount of light intercepted by the module.

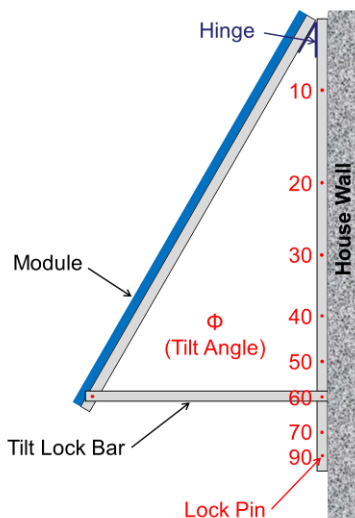


Figure 2: Drawing of module wall mount.

A module mount, accommodating a 60-cell Suniva module is shown in Fig. 3. The module aluminum frame is connected to a ground rod. A feed-through carries the module positive and negative leads, along with the ground wire, through the wall and to the remainder of the system components inside the home office. The module mount can also be free-standing, as illustrated in Fig. 4.

2.3 Load Demands

Power requirements for various loads that could be used with the solar generator are listed in Table II. These values were measured with the AC display (Kill-A-Watt). With a 600 Wh limit (50% depth of discharge), the daily maximum usage can be determined. For example, the LCD color TV (by itself) could run for 20 hours/day, while the refrigerator could run for 4 hours/day. Weights of system elements are given in Table III.



Figure 3: Module (255 W, 60-cell) mounted on back wall of house and inclined 40° from the horizontal (tilt appropriate for spring season).



Figure 4: Module mounts used in free-standing mode.

Table II: Measured AC power requirements for various loads.

Load	Power (W <sub>ac</sub> )
LED lamp (800 lumens)	16
18-inch (diagonal) LCD color TV	31
Ipod music system	11
Kitchen refrigerator	153
Treadmill	116
Hand power drill	152
Hand power saw	675
Gas Furnace (electric starter and blower)	509

Table III: Weights of system elements.

Element	Weight (kg)	Weight (pound)
Battery	28	62
Module	19	41
Module mount	20	44
Electronic controls	11	25

3 SYSTEM PERFORMANCE

System performance (Wh of energy delivered to load per day) depends on the efficiency of each component in the system, from module to inverter. Performance also depends on the orientation of the module for intercepting

sunlight and on atmospheric conditions (primarily cloud cover and air temperature). Efficiency parameters have been measured or assessed from vendor data, and the impact of module orientation has been quantified. As a result, a prototype solar generator has been implemented to power a home office.

### 3.1 Component Efficiencies

The efficiency of the charge controller was first assessed with the charge controller in an operating system as shown in Fig. 1. The DC display has the ability to monitor instantaneously the current and voltage input to the charge controller from the module and the current and voltage output to the battery from the charge controller. Hence, the ratio of power output from the charge controller to power output from the module can be determined. Typical and reproducible operating data are given in Table IV, where it is shown that the measured efficiency for the charge controller is 90%.

**Table IV:** Measured module power at  $P_{mp}$  and charge controller power, with power efficiency ratio for charge controller.

Parameter	Value
$V_{module}$	26.1 V <sub>dc</sub>
$I_{module}$	8.1 A <sub>dc</sub>
$P_{module}$	211 W <sub>dc</sub>
$V_{controller}$	12.2 V <sub>dc</sub>
$I_{controller}$	15.6 A <sub>dc</sub>
$P_{controller}$	190 W <sub>dc</sub>
Power Ratio	90 %

Note that the action of the charge controller is to nearly double the charging current available from the module (8.1 A) to send to the battery (15.6 A). The maximum charging current available from the controller is 20 A. If operational conditions (e.g., high light intensity, low temperature) are such that more than 20 A might be expected from the controller, the controller responds by departing from MPPT in order to maintain its output current at 20 A. During testing, such conditions have prevailed from time to time, and battery charging currents from the controller as high as 20 A have been observed. The battery chosen for this system (Lifeline GPL-27T) can accommodate charging currents of this magnitude - even up to 80 A, per manufacturer's data. A similar action of the charge controller occurs as the battery charge state progresses from "bulk" (battery accepts full current from the charger) to "acceptance" (battery accepts only that current required to keep the battery voltage at 14.5 V) to "float" (battery accepts only that current required to keep the battery voltage at 13.5 V). MPPT is utilized in the bulk charge mode, but the controller departs from MPPT and slides down the module I-V curve toward  $V_{oc}$  (less current) in the acceptance and float modes as the battery approaches a fully-charged state.

Similar efficiency measurements were performed for the inverter. DC current from the battery into the inverter was measured by means of an amp-clamp and battery voltage was measured by the charge controller. AC voltage and current from the inverter to the load were measured by the Kill-AWatt meter. Typical and reproducible values are given in Table V which shows an inverter efficiency of 93% while supplying a relatively

high power of 433 W to the load. Since the system is designed for a total daily output energy of 600 Wh in order to limit the depth of discharge of the battery to 50%, the system would be able to deliver 433 W of power for only about 1.4 hours continuously.

**Table V:** Measured battery power (inverter input) and inverter power, with power efficiency ratio for inverter.

Parameter	Value
$V_{battery}$	12.2 V <sub>dc</sub>
$I_{battery}$	38.0 A <sub>dc</sub>
$P_{battery}$	464 W <sub>dc</sub>
$V_{inverter}$	121 V <sub>ac</sub>
$I_{inverter}$	3.58 A <sub>ac</sub>
$P_{inverter}$	433 W <sub>ac</sub>
Power Ratio	93 %

Multiplying the charge controller efficiency (90%) by the inverter efficiency (93%) gives an upper bound on system efficiency at 84%. However, the module output can also differ from its rated value under standard test conditions (STC) of 1-sun and 25°C. In particular, elevated module temperatures will decrease module output. The manufacturer's module temperature coefficient is -0.42%/°C for power. The normal operating cell temperature (NOCT) is given as 46°C, which is 21°C above standard test conditions. Hence the effective module efficiency under normal operating conditions at 1-sun insolation is  $(1 - 0.0042)^{21}$ , or 92%. Similarly, the real battery efficiency (Ah out/Ah in) is less than 100%. The manufacturer gives a battery efficiency range of 91% to 98% depending on details of the discharge. Thus, assuming a module operating at NOCT and a battery operating at the low end of its efficiency range, the overall efficiency relative to a module operating at STC is given as  $0.92$  (module)  $\times$   $0.90$  (charge controller)  $\times$   $0.91$  (battery)  $\times$   $0.93$  (inverter) = 0.70. This means that the solar generator system with a 255 W module, operating on the equivalent of 4.2 hours at 1-sun (yearly average), can deliver 750 Wh ( $255 \text{ W} \times 4.2 \text{ h} \times 0.70 = 750 \text{ Wh}$ ) of energy to the load (daily average). Since this value exceeds the self-imposed limit of 600 Wh to preserve the life of the battery, this analysis suggests the system will operate as designed.

### 3.2 Light Acceptance

In addition to individual components performing as required, the module must also be oriented properly to intercept as much light as possible within the limitations of its fixed position. A methodology was developed to determine the fraction of sunlight intercepted by the module over the course of a day. This permits an assessment of the equivalent number of hours with 1-sun reaching the module. The location of the sun as a function of time is needed, along with a vector representation of the module orientation.

By measuring the length of a shadow cast from a thin vertical rod (19 mm diameter wooden dowel, 1016 mm long) as well as the projection of that shadow along an east-west line, a unit vector in the direction of the sun ( $u_{sun}$ ) can be defined. Similarly, a unit vector perpendicular to the module face ( $u_{module}$ ) can be constructed. In this case, the module (S120) is facing due

south and is inclined from the horizontal at the local latitude angle (41.4°), so  $u_{\text{module}} = 0x - 0.661y + 0.750z$ . The dot product of  $u_{\text{sun}} \cdot u_{\text{module}}$  then gives the cosine of the angle between the sun and the module, or the fraction of light intercepted by the module. For example, at a time of 13:00 on April 5, 2013, the unit vector pointing toward the sun is  $u_{\text{sun}} = 0.054x - 0.564y + 0.824z$ . The dot product ( $u_{\text{sun}} \cdot u_{\text{module}}$ ) is then 0.991, so 99.1% of the sunlight is intercepted by the module at that time. This high value indicates the module is well oriented for the given time of year. Such data for a particular day (April 5, 2013) is shown in Fig. 5 (Dot Product points), indicating a peak at about 13:00 (daylight savings time).

Superimposed on the Dot Product data of Fig. 5 is a direct measurement of light intensity (Suns) during the day. Light intensity was measured as the short-circuit current output from a calibrated silicon photosensor placed in the plane of the module. Note that the Suns data curve replicates the Dot Product data curve reasonably well, with a peak at about 1.1 suns. This shows that light intensity striking the module can exceed 1 sun near midday on a clear day. The overshoot of the Suns curve relative to the Dot Product curve near its peak may be a result of sunlight traveling through an air mass less than 1.5 at that time. An undershoot during the early morning and late afternoon times may be the result of light traveling through an air mass greater than 1.5, thereby suffering greater absorption.

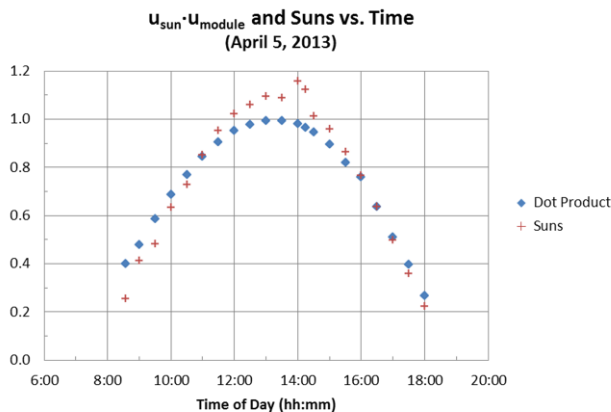


**Figure 5:** Fraction of sunlight intercepted by module from geometrical considerations (Dot Product) and measured light intensity in the plane of module (Suns).

The overall good agreement between the measured light intensity (Suns) and the inferred fraction of sunlight intercepted (Dot Product) suggests the Dot Product method is a valid means for assessing the solar resource on a clear day. By extrapolating the dot product curve to zero at the two extremes and integrating over the full curve, an assessment of the equivalent number of 1-sun hours can be made. For the data of Fig. 5, that value is 7.9 h.

The module temperature measured at the back of the module by an IR sensor was 35.7°C near the peak of Fig. 5. This is 10.7°C above STC, so the module power is then 96% of the STC value because of this elevated temperature. An estimate of the total energy which could be delivered to the battery is then given by:  $255 \text{ W} \times 7.9 \text{ h} \times 0.96 \times 0.90 = 1740 \text{ Wh}$ . This includes

controller efficiency (0.90) but takes battery efficiency to be 1. This estimate is appropriate for a cloud-free, relatively cool day (air temperature about 8°C).

### 3.3 Power Delivered to Battery

With the estimate of 1740 Wh of energy that could be delivered to the battery under the (near ideal) test conditions given above, it is necessary to measure the actual energy delivered to the battery in real-world conditions. This was done with the module (S120) mounted to the back wall of the home office, as shown in Fig. 3. Because of the orientation of the house wall, the module was facing not due south at a 41° tilt (Fig. 5 data), but southward with a 40° tilt from the horizontal. The base of the module was oriented 27° north of the east-west line instead of along the ideal east-west line. With this (slightly) non-ideal module orientation, the power delivered to the battery for the system of Fig. 1 was logged using a Universal Communication Module from Blue Sky Energy. This permitted the acquisition of the maximum current from the charge controller to the battery and the maximum battery voltage during each 6-minute interval. The product of these two maxima is a reasonable representation of the power delivered to the battery during that 6-minute interval. This power is plotted in Fig. 6 as a function of time on May 13, 2013.

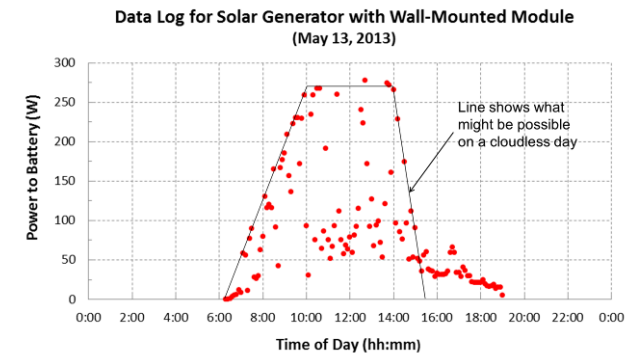


**Figure 6:** Power from module delivered to battery as a function of time of day.

Note that the data of Fig. 6 are scattered because of cloud variability throughout the day. The cumulative charge delivered to the battery for the day, as recorded from the charge controller by the IPN-ProRemote, was 47 Ah. Assuming a nominal battery voltage of 12 V, this corresponds to the delivery of 564 Wh of energy to the battery – which is close to the 600 Wh design target. The significant dropoff of power after 15:00 is due to a partial shading of the module from the eaves of the roof.

It is clear from the data of Fig. 6 that some points define the maximum power possible over the course of the day. The solid black line connects these points to show what might be possible for a cloudless day. The integrated area beneath the black lines gives an estimate of the total energy that could be delivered to the battery on such a day as 1800 Wh. Note that this value is in reasonable agreement with the 1740 Wh that was obtained from Fig. 5 during a cloudless day.

Experience with the solar generator has shown that the charge delivered to the battery on a typical day is about 50 Ah, consistent with the 50% depth of discharge desired. However, during the March through September,

2013 time frame, extremes in daily battery charge have ranged from 2 Ah (extremely cloudy and raining) to 113 Ah (cloudless and cool). These correspond to energy delivered to the battery ranging from 24 Wh to 1360 Wh.

### 3.4 Home Office Implementation

The full system of Fig. 1 with the module wall mount of Fig. 3 has been assembled to power a home office. The loads needed for the home office are shown in Fig. 7 and include a laptop computer, modem, router, black & white printer and color printer/scanner. The module frame is connected electrically to a ground rod at the base of the outside wall. Along with the positive and negative module leads, this ground is carried through the wall feed-through to the components inside the office in order to establish the chassis ground. The home office has been in use without incident for about six months powered by the solar generator. Only rarely is the battery charger called upon to supplement the charge delivered to the battery by the charge controller.



**Figure 7:** Home office (modem, router, laptop computer, black & white printer and color printer/scanner) powered by solar generator with module mounted on opposite side of back wall.

## 4 OPPORTUNITY FOR IMPROVEMENT

It is clear from IR measurements of the back surface of the module of Fig. 3, which is powering the remaining components of the solar generator, that the module operates at a temperature considerably above the ambient air temperature. For example, on April 22, 2013 at 12:56, the module was producing 244 W (9.1 A at 26.8 V) with the back surface at 46°C and outdoor air temperature at 12°C. This temperature difference of 34°C degrades the module power output to  $(1 - 0.0042)^{34} = 0.87$  of what it would be with no temperature rise above ambient. This means that although the module was producing a respectable 244 W, with no temperature rise above ambient it would have been producing 280 W.

In an effort to recover some of this “lost” power, a heat transfer analysis was undertaken to estimate the potential benefit of passive cooling fins thermally bonded to the back of the module. The calculation was based on

$$dQ/dt = h \times A \times \Delta T \quad (1)$$

where  $dQ/dt$  is the heat flow from the back of the module driven by a temperature difference ( $\Delta T$ ) between the module and the ambient air,  $h$  is the convective heat transfer coefficient, and  $A$  is the area of the module surface.

In addition to convective heat transfer, radiative heat transfer is also important. Radiative heat transfer can be calculated using an effective heat transfer coefficient ( $h_r$ ) where surface emissivity ( $\epsilon$ ) plays a role. Considering both the front (f) and back (b) module surfaces, as well as heat transfer by both convection (c) and radiation (r), Eq. 1 is generalized to:

$$dQ/dt = (h_{rf} \times A_{rf} + h_{cf} \times A_{cf} + h_{rb} \times A_{rb} + h_{cb} \times A_{cb}) \Delta T \quad (2)$$

where  $h_{rf}$  and  $h_{rb}$  are radiative heat transfer coefficients from the front and back surfaces,  $h_{cf}$  and  $h_{cb}$  are convective heat transfer coefficients from the front and back surfaces,  $A_{rf}$  and  $A_{rb}$  are the front and back surface areas for radiative heat transfer, and  $A_{cf}$  and  $A_{cb}$  are the front and back surface areas for convective heat transfer.

Representative results of the heat transfer calculation are summarized in Table VI. Note that improved cooling is associated with increased rear surface area (factor of 6.4) by virtue of cooling fins on the back. Calculated reduction in  $\Delta T$  is from 27°C to 12°C. This is based solely on increased surface area, assuming the same convective heat transfer coefficients remain in effect with and without cooling fins. Calculated improvement in module power output with rear passive cooling is 16 W, or 6.0% of STC power for the case considered. These encouraging estimates suggest efforts to increase module power output by passive cooling are warranted.

**Table VI:** Summary of assumed heat transfer parameters and calculated temperatures, power loss, and encapsulated cell efficiencies for a standard module with planar front and back and for a module with cooling fins applied to the back for passive cooling.

Parameter	Standard Module	Module with Passive Cooling
$\epsilon_f$ (glass)	0.84	0.84
$h_{rf}$ (W/m <sup>2</sup> -K)	6.8	6.8
$A_{rf}$ (m <sup>2</sup> )	1.49	1.49
$h_{cf}$ (W/m <sup>2</sup> -K)	7.3	7.3
$A_{cf}$ (m <sup>2</sup> )	1.49	1.49
$\epsilon_b$ (tedlar or aluminum sheet)	0.95	0.09
$h_{rb}$ (W/m <sup>2</sup> -K)	6.8	6.8
$A_{rb}$ (m <sup>2</sup> )	1.49	1.49
$h_{cb}$ (W/m <sup>2</sup> -K)	7.3	7.3
$A_{cb}$ (m <sup>2</sup> )	1.49	9.54
$dQ/dt$ (W-total)	1080	1080
$[dQ/dt]_r$ (W-radiative)	490	110
$[dQ/dt]_c$ (W-convective)	590	970
$\Delta T$ above ambient for NOCT (°C)	27	12
$(1 - 0.0045)^{\Delta T}$	0.885	0.947
Module Power (265 W at STC)	235	251
Power lost by $\Delta T$ (W)	30	14
Encapsulated cell efficiency at STC (%)	18.5	18.5
Encapsulated cell efficiency lost by $\Delta T$ (%)	2.1	1.0
Effective cell efficiency at NOCT (%)	16.4	17.5

## 5 SUMMARY

A simple solar generator system, built around a single production-style c-Si module, a single lead-acid battery, a single charge controller with maximum power point tracking, and a pure sine wave inverter, was designed, evaluated, and put into operation supplying power to a home office. The system included a versatile module mount which can be used to attach the module to a vertical wall while allowing a range of tilt angles, or as a stand-alone module support. The efficiency with which power can be moved through the charge controller and the inverter was measured to be 84%. A simple method to track the position of the sun in the sky was developed, which allowed a means for also tracking the fraction of sunlight intercepted by a module with fixed tilt over the course of the day. The typical daily charge delivered to the battery was observed to be approximately 50 Ah, corresponding to an energy delivery of 600 Wh. However, measured data suggest the energy delivery to the battery could be as high as 1400 - 1800 Wh on a cloudless, cool day. Module heating up to 34°C above ambient was observed, with its concomitant loss in module power. Heat transfer calculations suggest this heating might be reduced to 15°C above ambient with the aid of passive cooling fins applied to the back of the module.

## 6 ACKNOWLEDGMENT

The authors gratefully acknowledge Mr. Charlie Grazioli for his expertise in constructing the module mounts and for installing the solar generator at the home office.

## 7 REFERENCES

- [1] I. Katic, P. H. Pedersen, and E. D. Jacobsen, "Stand-Alone Solar Powered Refrigeration Systems with PCM or Battery Storage – Test Results, Field Experience and Perspectives," Proceedings of the 27<sup>th</sup> European Photovoltaic Solar Energy Conference, pp. 4291-4293 (2012).
- [2] P. G. Nikhil and D. Subhakar, "Sizing and Parametric Analysis of a Stand-Alone Photovoltaic Power Plant," IEEE Journal of Photovoltaics, vol. 3, no. 2, pp. 776-784 (2013).
- [3] NREL Renewable Resource Data Center - PVWatts, see <http://www.nrel.gov/rredc/pvwatts> for US zip code 15857.